Front. For. China 2007, 2(3): 350–354
DOI 10.1007/s11461-007-0057-5

RESEARCH ARTICLE

**WANG Zheng, ZHU Dianxiang**

# Power spectrum density and experimental modal analysis of wide belt sander applied in domestic wood industry



**Abstract** This paper took the upper-lower wide belt sander B229 with four-feet wide belts, manufactured in China, as the study target. By means of framework dynamic design, we study its vibration characteristics by commencing from the place having horizontal defects and used experimental modal analysis (EMA) and power spectrum density (PSD) to observe the sanding parts and the whole machine, respectively. In the modal test, we mainly adopted the cross spots testing method to get the frequency response function of the fixed spots to every excitation vibration spot, then applied the SISO frequency response function and the frequency response function fitting method to identify and complete parameter recognition, respectively. The typical frequency response function chart of the whole machine and its sanding parts, as well as its second-order mode charts of contacting roller, were obtained. Through PSD analysis, we can get the amplitude-frequency spectrum and drive frequency.

**Keywords** experimental modal analysis (EMA), power spectrum density (PSD), wide belt sander, dynamic design, frequency response function, modal parameters

## 1 Introduction

Modern technologies, especially with the rapid development of aviation, astronautics, and oceanographic engineering, promote vibration technology dramatically with regards to research and application. Modal analysis is an important method in the study of structure dynamic design and equipment failure diagnosis. It is also applied in system identification in the realm of system vibration. Experimental modal analysis (EMA) and power spectrum density (PSD) technology are important branches of vibration engineering. Their reliable test results have become effective standards of product performance assessment. The methods concluded from structure dynamic design, breakdown diagnosis, and condition monitor method causes the modality analysis to become the structural design's important basis.

In view of the fact that the wood industry is always the main customer of belt grinding machinery, many domestic sander manufacturers have, in recent years, realized that mechanical device vibration situation influences the technology qualitative indices, the economic indicator, and consequently, machining precision, machine life, and productivity. Thus, they should develop the study of structural design from machinery dynamic characteristics. The vibration quantity reflects the quality of the wide band type sander sensitivity. However, the reason for vibration breakdown changes.

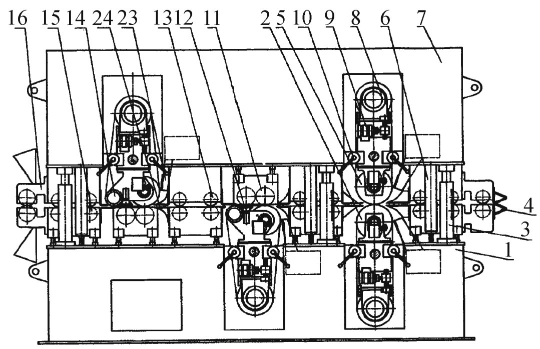


**Fig. 1** Front view of the wide belt sander B229, four feet in width and four grinding shelf, applied in wood industry
1) Lower shelf of machine; 2) lower coarse grit roller; 3) oil vat; 4) limited board device; 5) upper coarse grit roller; 6) thickness regulator; 7) upper shelf of machine; 8) tighten roller; 9) swing gas vat; 10) tight lock handle; 11) reverse stress roller; 12) grinding pillow; 13) upper feeding roller; 14) guiding roller; 15) lower feeding roller; 16) cleaning and outlet roller; 23) main mouth of dirt collecting; 24) guiding board.

Translated from *Scientia Silvae Sinicae*, 2005, 41(6): 132–137 [译自: 林业科学]

WANG Zheng (✉), ZHU Dianxiang
College of Wood Science and Technology, Nanjing Forestry University, Nanjing 210037, China
E-mail: wangzheng63258@163.com

## 2 Experimental modality analysis theory

In engineering, the movement differential equation of a linear vibration system is

$$[M]\{\ddot{x}\}+[C]\{\dot{x}\}+[k]\{x\}=\{f(t)\} \tag{1}$$

where $[M]$ is the mass matrix ($n \times n$), positive definite matrix; $[K]$ the stiffness matrix ($n \times n$), positive semidefinite matrix; $[C]$ the damping matrix ($n \times n$), positive semidefinite matrix; $\{\ddot{x}\}$ the acceleration matrix ($n \times 1$); $\{\dot{x}\}$ the velocity vector ($n \times 1$); $\{x(t)\}$ the displacement vector ($n \times 1$); $\{f(t)\}$ the excitation power vector ($n \times 1$), and $n$ the freedom degree (Ying, 2002).

The transfer function of a multiple-degrees-of-freedom system can spread out the linear superposition of many single-degree-of-freedom systematic transfer functions. This is the core of modal analysis. The modal superposition of $n$-order systematic transfer function is

$$H(s)=\sum_{r=1}^{n}\frac{\phi_r\phi_r^T}{m_r s^2+c_r s+k_r} \tag{2}$$

where $\phi_r$ is the vector under the $r$-order modality. For undamped and proportion damping system, $\phi_r$ is the real number. For the structure damping and the general viscous-damping system, $\phi_r$ is the plural number.

The frequency response function is the foundation of modal parameter recognition. The overall system frequency response function matrix modality $H(\omega)$ expansion is

$$H_{ij}(\omega)=\frac{X_i(\omega)}{F_j(\omega)}=\sum_{r=1}^{n}\frac{\phi_{ri}\phi_{rj}}{m_r[(\omega_r^2-\omega^2)+j2\xi_r\omega_r\omega]} \tag{3}$$

In type, $\phi_{ri}$, $\phi_{rj}$ is the vibration shape of a little place under $i, j$ order model form, $m_r$ for model form quality, $\xi_r$ is model form damping proportion, $\omega_r$ is $n$th natural frequency (Hu et al., 2002), $\omega_r^2=\frac{k_r}{m_r}$, $\xi_r=\frac{c_r}{2m_r\omega_r}$.

When $F_i=\{m_r[(\omega_r^2-\omega^2)+j2\xi_r\omega_r\omega]\}^{-1}$, then

$$H(\omega)=\sum_{i=1}^{m}F_i\begin{bmatrix}\phi_{1i}\phi_{1i} & \phi_{1i}\phi_{2i} & \cdots & \phi_{1i}\phi_{ni}\\ \phi_{2i}\phi_{1i} & \phi_{2i}\phi_{2i} & \cdots & \phi_{2i}\phi_{ni}\\ \vdots & \vdots & \vdots & \vdots\\ \phi_{ni}\phi_{1i} & \phi_{ni}\phi_{2i} & \cdots & \phi_{ni}\phi_{ni}\end{bmatrix} \tag{4}$$

In the frequency response function, the element of matrix line $l$ and row $p$, presents the frequency response function of this point. By this transfer function matrix, if any row of transfer function through the conductance survey was obtained (for example row $j$), we can know

$$\{H_j\}=\sum_{i=1}^{m}F_i\phi_{ji}\{\phi_{1i},\phi_{2i},\ldots,\phi_{ni}\}^T \tag{5}$$

has contained all information of the modal matrix (Fu, 2000). In view of this, we can get the various order modal frequency, the damping, and the modality by measuring some line or row (Cao et al., 2001).

## 3 Test equipment and test method

### 3.1 Wide belt sander and place for testing

Table 1 shows the main technical parameters of this wide belt sander. The tested place was in the medium density fiberboard (MDF) production line of Jieda Wood Industry Limited Company, Guannan, Jiangsu Province, China.

### 3.2 Measuring instrument

Agilent 35670 dynamic signal analyzer, HP 320 workstation, PCB 308B02 ICP accelerometer, PCB SP205 exciting hammer (weight 2 kg), PCB LIXIE (weight 5 kg, with ICP force sensor) and "MODAL 3.0 SE system" were used in the structural measurement system. This software, including the geometry characteristics matched with this prototype, can establish many kinds of coordinate systems that can be divided into many sub-structures. It also has many kinds of fitting methods and the structure modality vibration can be shown real-time on the screen by three-dimensional animation.

### 3.3 Test system diagram

See Fig. 2.

### 3.4 Testing points arrangement

First determine the position of the detecting point, and then determine the number and direction of drop-points and each drop-point position.

#### 3.4.1 Grinding shelf part

The exciting and the sensor positions were located on the touch roller, guiding roller and bearing base. Figure 3 shows

**Table 1** Main technological parameters list of the wide belt sander B229 in wood industry

| Number of the grinding shelf /entries | Range of the finished product thickness /mm | Machining precision /mm | Sand belt rate /(m·s$^{-1}$) | Material delivery rate /(m·min$^{-1}$) | Weight /t | Motor power of the grinding shelf /kW |
|---|---|---|---|---|---|---|
| 4 | 2.5–40 | ±0.1 | 26 | 4–24 | 27 | 75 × 2, 55 × 2 |

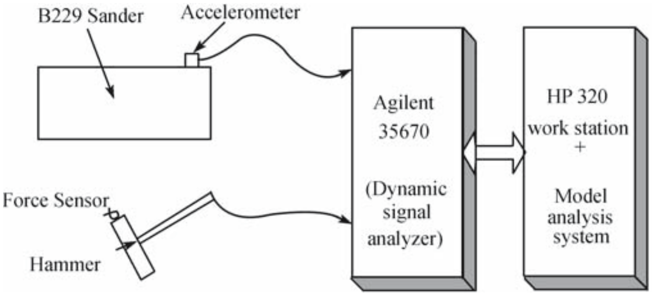


**Fig. 2** Testing system frame diagram

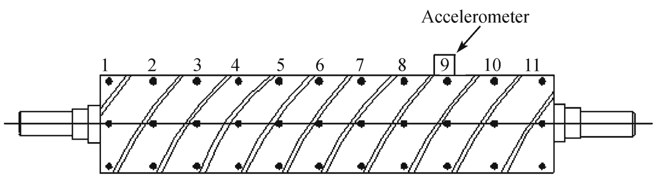


**Fig. 3** The distribution of exciting and sensor positions on the touch roller

the exciting and sensor positions on the touch roller. A 1.4-m long touch roller and guiding roller were divided into 10 equal segments.

3.4.2 Machine shelf

The sensors were located in the front and rear of the bearing base. The signal of vibration responding from the whole machine was acquired by exciting the upper-frame.

3.5 Testing methods

The machine was excited by the hammer. The acceleration signals were measured at the same response position (such as the ninth point in Fig. 3) while exciting position varies each time, and the frequency response function of the machine was obtained by the single input single output (SISO) method.

## 4 Results and discussion

4.1 Typical frequency response function

Frequency response curve by five times of the upper-frame (F) in rear bearing base (R) is shown in Fig. 4. Exciting force applied to the upper-frame and response of the front and rear of the bearing base are listed in Table 2.

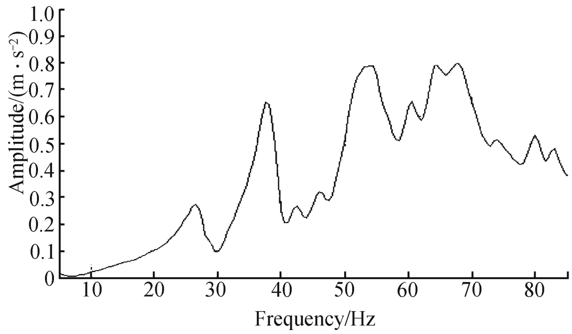


**Fig. 4** Frequency response curve by 5 times of the upper-frame

4.2 Frequency response function of sand shelf

The measured response and exciting force applied to the bearing base and touch roller are listed in Table 3. Frequency response curves of the bearing base and touch roller are shown in Figs. 5 and 6, respectively.

4.3 Frequency identified modes

Frequency identified modes are shown in Table 4.

4.4 Modal shapes

The first and second bending modes are shown in Figs. 7 and 8, respectively.

**Table 2** The list of exciting force applied to the upper-frame and response of the front and rear of the bearing base

| Positions for test | Main frequency components /Hz |
|---|---|
| Forced to the up sander frame and response to forward and front axletree seats | 26.5, 38.0, 69.5 |
| Forced to the up sander frame and response to forward and back axletree seats | 26.5, 38.0, 69.5 |
| Forced to the up sander frame and response to forward and back axletree seats (zoom out spectrum) | 26.5, 38.0, 69.5 |

**Table 3** The list of the measured response and exciting force applied to the bearing base and touch roller

| Positions for test | File name | Main frequency components /Hz |
|---|---|---|
| Forced to the front axletree seat and response to the front axletree seat | b1 | 108, 141.5 |
| Forced to the back axletree seat and response to the front axletree seat | b2 | 108, 142, 163 |
| Forced to the front axletree seat and response to the back axletree seat | b3 | 178, 221, 300 |
| Forced to the fourth dot and response to the 1st dot in the touching roller | ab1 | 45.0, 48.25, 83.25 |
| Forced to the fourth dot and response to the 2nd dot in the touching roller | ab2 | 45.0, 48.25, 83.25 |

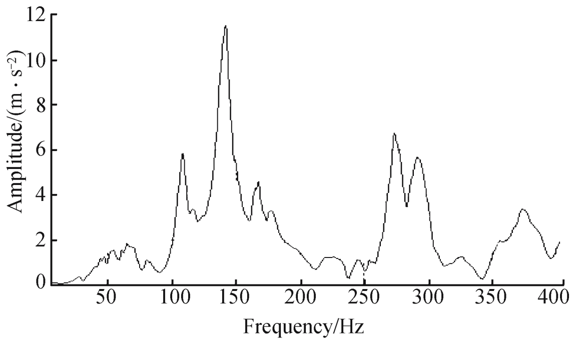


**Fig. 5** Frequency responses curves of the bearing base and touch roller

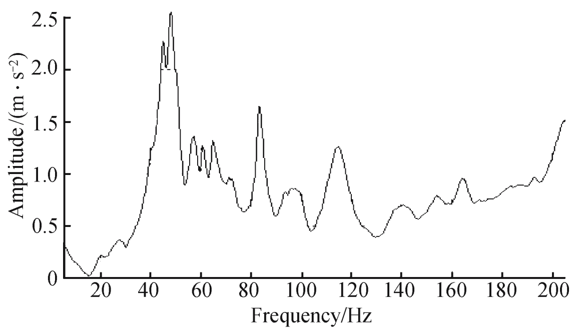


**Fig. 6** The amplitude-frequency curve drawing forced to the 4th dot and response to the 2nd dot in the touching roller

**Table 4** The list of the nature frequency with mode form

| The name of testing object | Rank number with mode form | The natural frequency with mode form /Hz | Damping ratio with mode form /% |
|---|---|---|---|
| Guiding roller | The first rank | 143.3 | 1.89 |
| Guiding roller | The second rank | 283.1 | 2.10 |
| Touching roller | The first rank | 45.0 | 1.40 |
| Touching roller | The second rank | 83.25 | 1.90 |
| Whole machine | The first rank | 26.50 | 5.10 |
| Whole machine | The second rank | 38.10 | 2.40 |

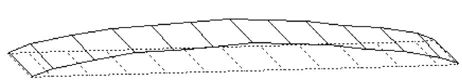

**Fig. 7** The first step mode of the touching roller (Natural frequency of 45.0 Hz, damping ratio of 1.4%)

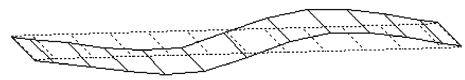

**Fig. 8** The second step mode of the touching roller (Natural frequency of 83.25 Hz, damping ratio of 1.9%)

## 5 Power spectral density (PSD) measurement

Power spectral density can reflect the frequency characteristics of stochastic vibrations. The PSD function takes the instantaneous vibration frequency in the envelope as the center frequency. Its shape is similar to a sharp pulse. Through the analysis of autopower spectral density for response signal (output), we can determine the frequency ingredient of drive signal (input) and so on. Therefore, after measuring the acceleration response from the autopower spectral density for wide belt sander B229, output characteristics of this system can be obtained. Its modality parameter had reflected the dynamic characteristics of this system.

Taking the analyses all round, we can get the primary frequency components of PSD for this machine under two conditions (Table 5). C1, C1a, C3, C2, C2a and C2b are the filenames of PSD in six different conditions. Obviously, when this sander's natural frequency is coupled with some primary frequency components in Table 5, resonance easily occurs, which can cause MDF to have cross-grained flaws.

The following figures reflect PSD of C1a, C2a and C3 (Figs. 9–11).

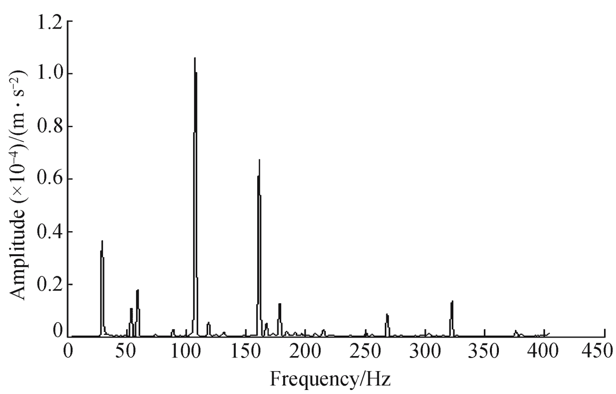


**Fig. 9** PSD drawing of the front axletree seat on load

**Table 5** Primary frequency components of PSD

| Measuring dot position | File name | Working state | Primary frequency components /Hz |
|---|---|---|---|
| The front axletree seat | C1 | No grind to MDF | 25, 29.5, 53.5, 89.0, 108, 161.5 |
| The front axletree seat | C1a | Grind to MDF | 25, 29.5, 50, 53.5, 59.5, 89, 100, 108 |
| The back axletree seat | C2a | No grind to MDF | 25, 29.8, 50.25, 53.7, 59.8, 100, 108 |
| The back axletree seat | C2b | Grind to MDF | 25, 29.8, 42.5, 50, 53.5, 59.5, 100, 108 |
| The motor seat | C3 | No grind to MDF | 25, 29.8, 50, 53.7, 59.5, 100 |

**Table 6** Measuring data of the eight sheets of MDF with cross-grained flaws

| Degree | 1 | 2 | 3 | 4 | 5 | 6 | 7 | 8 | $\frac{1}{n}\sum_{i}^{n}$ |
|---|---|---|---|---|---|---|---|---|---|
| Period distance /mm | 217.05 | 217.05 | 217.00 | 217.00 | 216.95 | 217.05 | 216.95 | 216.95 | 217.00 |

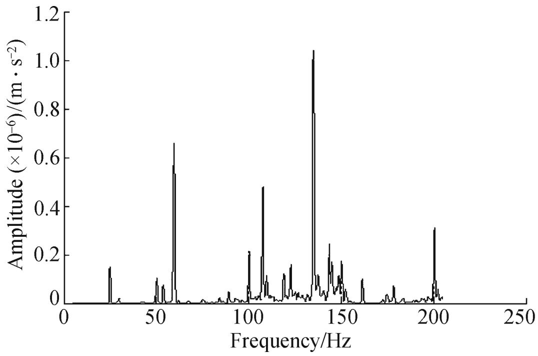


**Fig. 10** PSD drawing of the back axletree seat on load

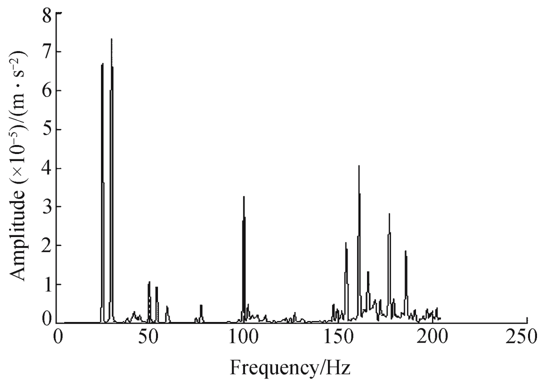


**Fig. 11** PSD drawing of the motor seat on load

## 6 Conclusion and suggestion

### 6.1 Analysis on cross-grained flaws of 8 sheets of MDF in three batches

The diameter of the touch roller was 0.345 m, and linear velocity of the sand belt was 27 m/s. Thus, the rotating speed of the rotor was about 25 r/min. We can conclude that an exciter existed at 25 Hz, and the exciter was the rotor. The average distance between each transverse line (217 mm) was calculated after modal testing. Frequency (26.11 Hz) of the transverse lines also can be determined.

Resonance of the sanding MDF occurred due to the coupling of the exciting frequency of the rotor (25 Hz) and the first natural frequency of the MDF (26.5 Hz). This phenomenon produced transverse lines on the face of the MDF, which was the major defect of the MDF. The first natural frequency of the driving rotor and the sand roller was 25 and 29.5 Hz, respectively. Resonance will not occur while the first natural frequency of the guiding roller and the touch roller is 143.3 and 45.0 Hz, respectively. Other exciters, such as cutting edge machine, had very low exciting energy, and did not lead to the resonance of the sanding MDF.

### 6.2 Suggestion

In addition to the static structure design, such as the machine installation, adjustment, dynamic balance to tighten roller, touch, and guiding roller, the designer also needs to pay attention to the dynamics design. Many kinds of methods will be useful to the dynamics design, such as the modal test. Focusing on the electric abrasive finishing machine (EAFM) design, there are four points we should pay attention to.

1) Adjust the power of the driving rotor. If possible, avoid resonance by altering the rotating speed of the rotor.

2) Apply sensitive methods to structural dynamics design. Because those parameters have significant influences on the mode shapes, and they are sensitive to the eigenvalues and eigenvectors, we suggest to modify the mass, stiffness and viscous damping attached to the part that has large deformations in some mode shapes. According to this EAFM, we can alter its natural frequency by modifying its stiffness and mass. Through this method, we can separate the lower natural frequency of the EAFM from the exciting frequency, and thus avoid the resonance phenomenon.

3) Using a frame structure made of tempered steel or mixed ore, which can bear large loads for reducing vibration effectively.

4) Pay attention to the environmental exciter, and install vibration reduction equipment.

## References

Cao S Q, Zhang W D, Xiao L X (2001). Vibration Structure Model Analysis—Theoretical, Experimental and Applied. Tianjin: Tianjin University Press (in Chinese)

Fu Z F (2002). Vibration Model Analysis and Identify Parameters. Beijing: China Machine Press (in Chinese)

Hu H Y, Sun J H, Chen H H (2002). Mechanical Shock and Vibration. Beijing: Aviation Industry Press (in Chinese)

Ying H Q (2002).Vibration and Noise of Modern Technology. Beijing: Aviation Industry Press (in Chinese)